


Microstructural and Mechanical Properties of Alumina (Al₂O₃) Matrix Composites Reinforced with SiC from Rice Husk by Spark Plasma Sintering

Shatumbu Thomas Alweendo ^{a*} , Oluwagbenga Temidayo Johnson ^{a,c}, Brendon Mxolisi Shongwe ^b,
Frank Paul Kavishe ^a, Joseph Olatunde Borode ^d

^aUniversity of Namibia, Department of Mining and Metallurgical Engineering, Ongwediva, Oshana, Namibia

^bTshwane University of Technology, Institute for Nano Engineering Research, Department of Chemical, Metallurgical and Materials Engineering, Pretoria, South Africa

^cUniversity of Johannesburg, School of Mining, Metallurgy and Chemical Engineering, Faculty of Engineering and the Built Environment, Department of Metallurgy, Johannesburg, South Africa

^dFederal University of Technology, Department of Metallurgical and Materials Engineering, Akure, Nigeria

Received: May 30, 2019; Revised: December 19, 2019; Accepted: January 10, 2020

Alumina (Al₂O₃) suffers from low fracture toughness and low bending strength which restrict its application in the industry for some advanced components. The incorporation of submicron SiC into Al₂O₃ matrix improves mechanical properties of the matrix. However, the high cost of SiC has delayed the industrial interest of synthesizing Al₂O₃-SiC composites. Rice husk, an agricultural waste material, is a potential source of low-cost SiC. Therefore, this study presents a simple approach to synthesizing SiC from locally sourced rice husk and using it to reinforce alumina. Rice husk was pyrolysed in a tube furnace under argon atmosphere at different temperatures (1000 °C – 1500 °C) and reaction times (60 – 120 min). Furthermore, Alumina powder was admixed with 5 – 20 vol% SiC derived from rice husk, and then sintered at temperatures between 1300 °C – 1600 °C by spark plasma sintering. Maximum yield of SiC was obtained from rice husk at 1500 °C and 120 min. Materials with theoretical densities higher than 95% were achieved for the sintered composites. The hardness of sintered composites reached a maximum of 20.2±1.4 GPa, while a maximum of 4.7±.7 MPa.m^{0.5} was obtained for the fracture toughness.

Keywords: Sintering, microstructure, X-ray diffraction, mechanical properties, rice husk, Silicon carbide.

1. Introduction

Alumina (Al₂O₃) displays a great variety of properties which are of fundamental as well as technological interest. Among these properties are low density, high chemical inertness, high compressive strength and good wear resistance. Due to these properties, alumina is used in the production of armor systems, abrasive materials, cutting tools, electronics, aero and automotive parts¹. In addition, alumina also finds application in the biomedical field as an implant material for artificial hip, knee, shoulder, elbow and wrist, as well as for replacing diseased, damaged and loosened teeth². Alumina, however, has some drawbacks: low fracture toughness, low bending strength and a low heat-resistance limit temperature for strength. These weaknesses limit the use of Al₂O₃ for some advanced applications³.

Studies show that the incorporation of a small amount of nano-sized silicon carbide (SiC) significantly improves the overall mechanical properties of the alumina matrix composite, particularly hardness and fracture toughness^{4,6}. The effect of nano-sized reinforcements on toughening of alumina ceramics was first reported by Niihara and Jeong⁷ who asserted that the addition of 5 vol% nano-sized silicon

carbide particles into an alumina matrix had improved its strength by changing the fracture mode from inter granular to intra granular. However, the overall cost of production of SiC in the industry is high due to the contributions of the high raw materials and energy cost⁸. The need to overcome this challenge has led to intense research on alternative techniques as well as sources of silicon carbide that are low-cost and renewable, among which rice husk has emerged as one of the promising candidates due to its finely dispersed carbon and silica that are in intimate contact and exhibit high activity with one another^{9,10}.

Silicon carbide (SiC) was first synthesized successfully from rice husk by Cutler in the early 1970's^{11,12}. Consequently, various techniques such as thermal plasma reactors¹³ gas furnaces¹⁴, thermogravimetry-differential scanning calorimetry (TGA-DSC)¹⁵ and hydrothermal carbonization¹⁶ were experimentally employed to synthesize SiC from rice husk with a high degree of success. However, the sophisticated nature of these techniques makes it difficult for large scale production of SiC from rice husk due to high maintenance requirements. Therefore, there is still a need for a simpler and more economic approach to the synthesis of silicon carbide (SiC) from rice husk and using it to reinforce alumina to produce a low cost high performance alumina matrix - SiC

*email: talweendo@unam.na

reinforced composite and comparing the results to other work that utilized SiC from other sources. The use of rice husk ash in metal matrix composites has been reported¹⁷⁻¹⁹. However, reports on the reinforcement of alumina with SiC from rice husk have not been found or perhaps not officially published. Therefore, the aim of this work was to synthesize SiC from rice husk and using it to reinforce alumina with a focus of producing a low-cost ceramic matrix composite.

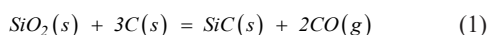
2. Materials and Methods

2.1 Preparation and characterization of starting materials

The rice husk used in this study was sourced from Ogongo rice project in Omusati region, northern Namibia. The as-obtained (raw) rice husk was washed with distilled water to remove dirt such as adhering sand and then dried in the sunlight for 12 h. After washing, a proximate analysis was done according to the ASTM standard D5373-02 (2007)²⁰ on 5g of raw rice husk pulverized in a Fritsch pulverisette 6 ball mill. Black ash was prepared by coking rice husk in a muffle furnace (635 HT) at 700 °C for 10 min before pyrolysis. The coking was carried out in sealed ceramic crucibles with a hole of 1 mm of diameter in the crucible cover to create an atmosphere deficient in oxygen. This step was necessary to convert organic matter into carbon. After coking, the sample was milled for 3 h in a Fritsch pulverisette 6 ball mill using 20 mm diameter stainless steel balls at 200 rpm and ball to powder ratio of 3:1. Alumina powder (99.8%) with a particle size of 3.5 microns (µm) from Labtech Suppliers, Windhoek, Namibia was used in this study.

2.2 Synthesis of SiC by pyrolysis of rice husk

Silicon carbide (SiC) was synthesized by pyrolysis of black ash (produced by the coking rice husk) in a tube furnace (THS 15-50-450). A mass of 5 g of the black ash were pyrolyzed at temperatures of 1000, 1300 and 1500 °C at a heating rate of 10 °C/min. The pyrolysis time was also varied at 60, 90 and 120 min. The process was done in an inert (argon) atmosphere flowing constantly at a rate of 2l/min to form pyrolysis products, which are SiC, unreacted SiO₂ and unreacted carbon. The pyrolysis products were calcined in a muffle furnace (Huster 635 HT) at 700 °C for 2 h in air to burn off the residual carbon. The calcined pyrolysis products were leached in hydrofluoric acid (HF) to remove any unreacted silica, while leaching in hydrochloric acid (HCl) was done to remove metallic oxide impurities as well as any residual carbon. After the treatments, the actual SiC mass was measured. The overall, stoichiometrically balanced formation reaction of SiC by carbothermal reduction of silica by carbon is given by Equation 1⁸.



From our previous study²¹, we established that there are 20% SiO₂ and 11% carbon by mass in the rice husk from proximate analysis. Therefore, the theoretical SiC mass was determined from the stoichiometric equation using the SiO₂ and C masses present in the rice husk used at different temperatures. The percentage yield was calculated using

Equation 2 after measuring the weight of the actual SiC obtained from rice husk.

$$\% \text{Yield} = \frac{\text{Actual SiC mass obtained}}{\text{Theoretical SiC mass}} \times 100 \quad (2)$$

2.3 Characterization of pyrolysis products

A Bruker D2 advance XRD analyzer was used to analyze the pyrolysis products before and after leaching to confirm the removal of impurities from the produced SiC powder. The D2 advance uses Co- α radiation produced at 40kV and 40mA, and the measurements were taken at 2 θ values ranging from 10°- 90° with step sizes of 0.02°. An FEI Quanta 400 FEG SEM/EDS machine was used for microscopic analysis of the treated pyrolysis products in terms of phase morphology.

2.4 Admixing alumina (Al₂O₃) with silicon carbide (SiC) from rice husk

Alumina and SiC powders were admixed in a planetary ball mill (Fritsch pulverisette 6) using 20 mm corundum balls at a ratio of 3:1 ball to powder, for 3 h. The powders were mixed in ratios of 5, 10, 15 and 20 vol% SiC in ethanol medium with the addition of dolapix CE 64 at 2 wt% as a dispersant, and then dried at 100 °C in an oven for 12 h.

2.5 Sintering of Al₂O₃-SiC composites

Spark plasma sintering (FCT HP-D5) technique was used to produce a consolidated Al₂O₃-SiC composite at different temperatures ranging from 1300 to 1600 °C at an interval of 100 °C and a ramp up of 250 °C/min for 5 min at 50 MPa pressure applied throughout the sintering cycle.

2.6 Density measurements

The densities of sintered composites were calculated using the Archimedes' principle as shown in Equation 3, where ρ_{water} is 1.0 gcm⁻³, m_s is the suspended mass of the samples, m_w is the saturated mass, and m_d is the dry mass.

$$\rho_s = (m_d \times \rho_{\text{water}}) / (m_s - m_w) \quad (3)$$

The theoretical densities of the composites were calculated using the rule of mixture method (3.95 g/cm³ and 3.21 g/cm³ for Al₂O₃ and SiC, respectively). The densification of the composites was calculated by dividing the experimental density by the theoretical density.

2.7 Microstructural characterization of sintered composites

All sintered samples were cut and polished to 1µm finish with diamond suspensions. An FEI Quanta 400 FEG SEM scanning electron microscope (SEM) equipped with an energy dispersive spectrometer was used to assess the microstructure of the polished samples. The elemental analysis was done using an energy dispersive spectrometer (EDS).

2.8 Mechanical properties of sintered composites

A Vickers hardness testing machine (MHV-1000A) was used to determine the hardness and fracture toughness of the sintered samples. The testing was performed by indenting the

sintered samples with a pyramid shaped diamond indenter under a test force of 5kg. Fracture toughness (K_{IC}) of the sintered materials was calculated using Equation 4, the Anstis' equation²².

$$K_{IC} = 0.016 \left(\frac{E}{H} \right)^{\frac{1}{2}} \times \frac{F}{C^{\frac{3}{2}}} \quad (4)$$

where F is the load in Newtons, c is the crack length from the centre of the indent to the crack tip in meters, E is the Young's modulus in GPa and H is the Vickers hardness in GPa.

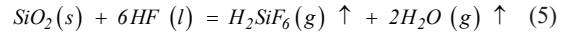
3. Results and Discussions

3.1 XRD analysis of pyrolysis products

Figure 1 presents the XRD spectra for the rice husk pyrolysed at 1300 °C and 1500 °C. Two major silica peaks can be observed at $2\theta = 22^\circ$ and 26.8° as shown in Figure 2a and 2b, respectively. These peaks imply that the amorphous silica had crystallized and transformed to β -cristobalite^{23,24}. It is evident that no silicon carbide (SiC) formed at 60 min for both pyrolysis temperatures. However, at 90 min, a small SiC peak was observed at $2\theta = 35.8^\circ$. The intensity of the SiC peaks increased further at 120 min, which indicates an increase in the yield of SiC from rice husk.

Figure 2 shows the composite XRD plot for leached pyrolysis products obtained at 1500 °C. The results revealed

that the leaching process has removed the unreacted silica and other oxide impurities. The hydrofluoric acid attacks the silica to form hexafluorosilicic acid vapour⁸ that effectively evaporates all silica from the pyrolysis products according to Equation 5. The main peak appeared at $2\theta = 42^\circ$ as opposed to that observed in Figure 1 at $2\theta = 35.8^\circ$. This variation was caused by the different anodes used as radiation sources for the XRD machines used. The spectrum in Figure 1 was obtained using an XRD machine with a Cu- α , while that in Figure 2 was obtained using Co- α radiation.



3.2 SEM analysis of silicon carbide (SiC) powder

Figure 3 presents an SEM image of the pyrolysis products after leaching. The image reveals that the obtained silicon carbide powder is in the form of whiskers and particles. The whiskers have diameters in the range 90 – 130 nm, while the particulates have diameters in the range of 60 – 110 nm. It is believed that the synthesis of SiC by carbothermal reduction of silica is a multi-stage, vapour-solid growth process that involves a series of chemical reactions which produce either particles or whiskers. SiC particles result from nucleation by reaction 6 with gas-solid interaction and whiskers grow by reaction 7.

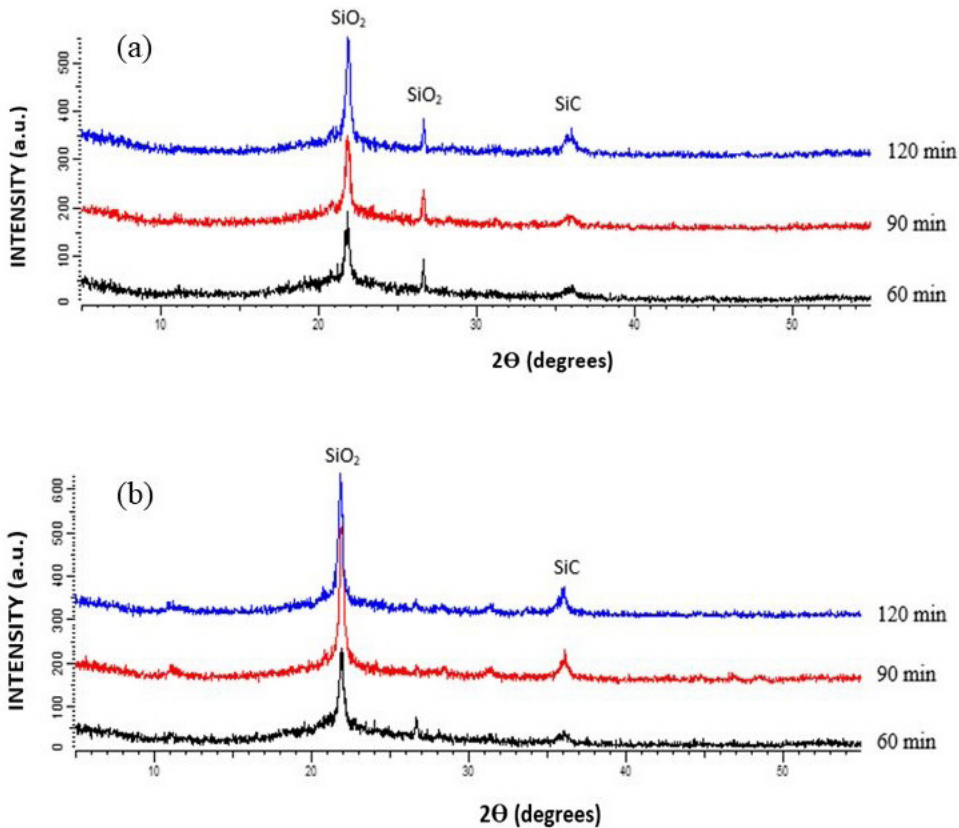
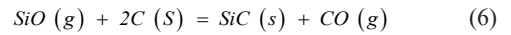


Figure 1: XRD spectra for rice husk pyrolysed at (a) 1300°C (b) 1500°C

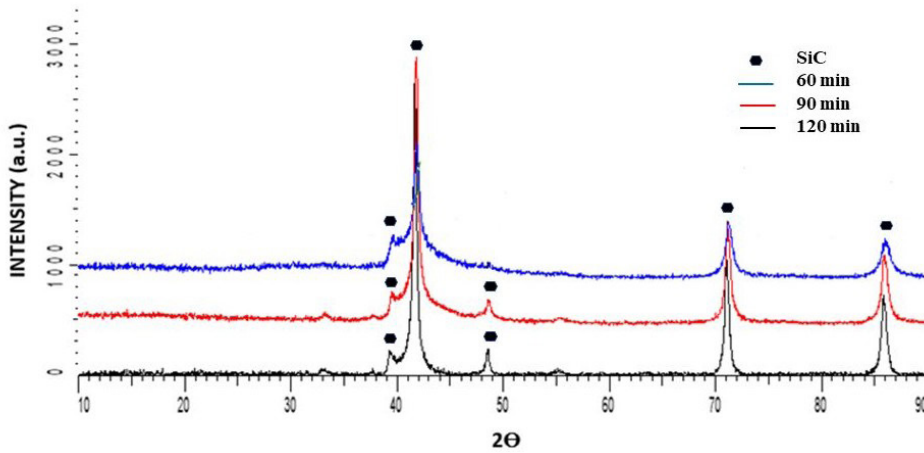


Figure 2: Composite XRD plot for leached pyrolysis products obtained at 1500 °C and different reaction times

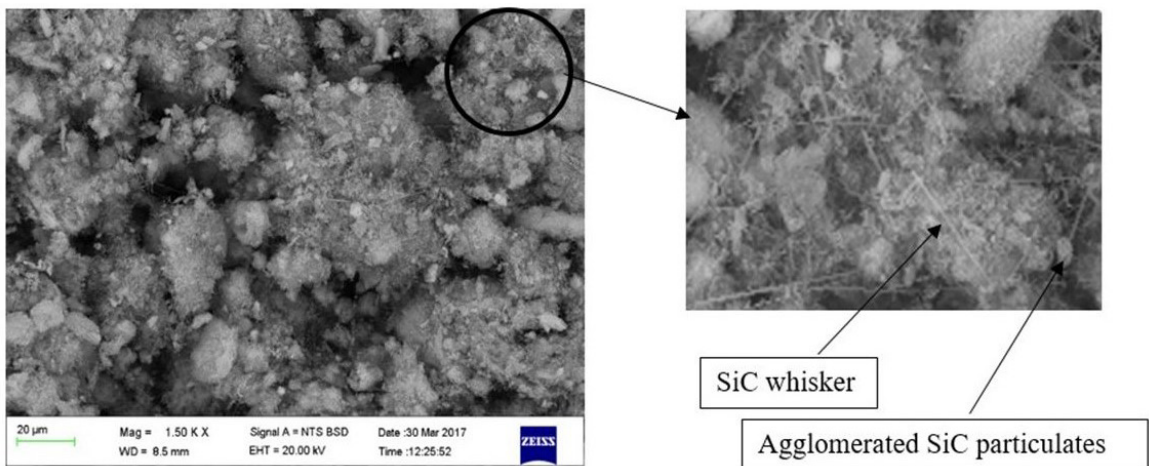
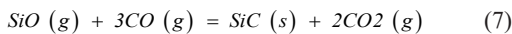


Figure 3: SEM image of SiC powder obtained from rice husk pyrolysed at 1500°C for 120 min



It is also believed that at temperature above 1450°C, some of the whiskers are converted to particulates via a process called coagulative formation of crystal particulates¹³.

3.3 Effects of temperature and time on SiC yield from rice husk

The effects of reaction time and temperature on the yield of silicon carbide from rice husk was investigated between 1300°C – 1500°C. The yield of silicon carbide was found to increase with an increase in temperature for all reaction times studied as shown in Figure 4. The maximum yield obtained was 69.2%.

3.4 Microstructural analysis of sintered Al₂O₃-SiC composites

Figure 5a presents SEM image of Al₂O₃-SiC materials doped with 20 vol% SiC sintered at 1500°C. The image displays a dense microstructure with some pores visible

within the matrix. This agrees with the density results in Figure 6, which reveal that this composite has a relative density of 96.4%. In addition, EDS spot analysis revealed that the light grey phase indicated by the arrows in Figure 5a is SiC as shown in Figure 5b. The SiC particles appear to be homogeneously distributed within the alumina matrix. Furthermore, XRD analysis of the composites reveal only Al₂O₃ and SiC peaks, which shows no secondary reactions between SiC and Al₂O₃ as shown in Figure 6.

3.5 Effects of sintering temperature and SiC composition on densification

The effects of sintering temperature and SiC composition on the densification of Al₂O₃-SiC composite are shown in Table 1 and presented in Figure 7, respectively. It was observed that the density of the composites increased with sintering temperature. This behaviour is expected because consolidation of powders during sintering occurs due to partial melting of powder particles, which is a temperature dependent phenomenon. Therefore, as the sintering temperature increases,

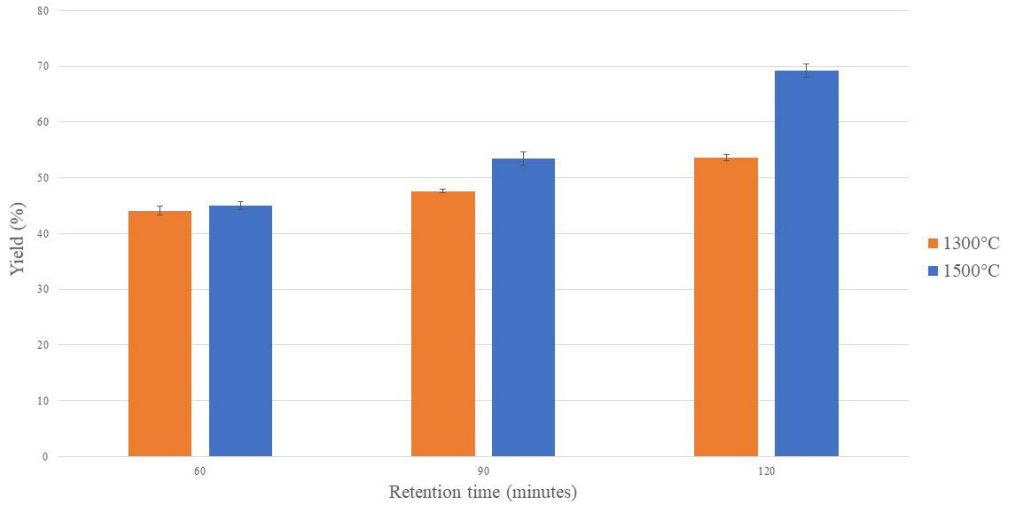


Figure 4: SiC yield as a function of retention time

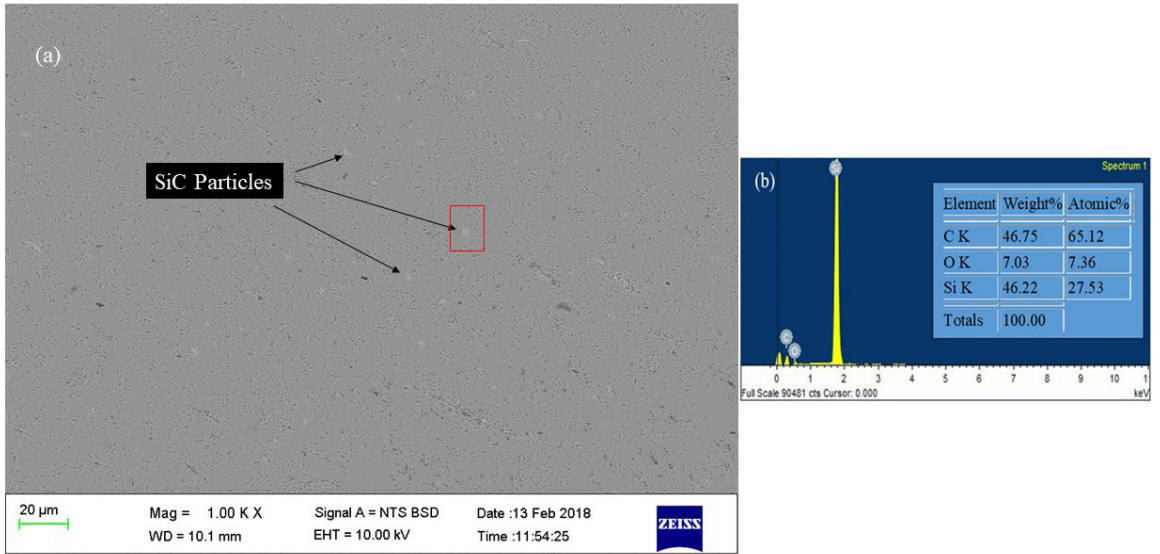


Figure 5: (a) SEM image of Al_2O_3 -20 vol% SiC composite sintered at 1500°C (b) EDS spot analysis results for Al_2O_3 -20 vol% SiC

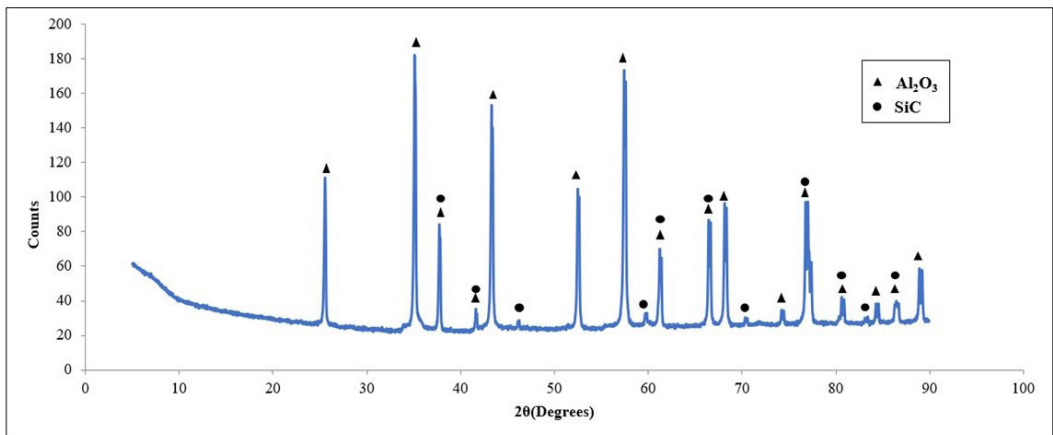


Figure 6: X-ray diffraction spectrum for Al_2O_3 -20 vol% SiC sintered at 1500°C showing only Al_2O_3 and SiC peaks.

the partial melting of powder particles in more pronounced which leads to better densification of the composites. From the table, it is evident that the incorporation of SiC into alumina matrix reduces the densification of alumina. This may be attributed to the poor sintering properties of the SiC phase. In a related study, Min et al.²⁵, successfully synthesized Sialon-SiC composites from kyanite tailings. They reported 1550°C as the optimum temperature for achieving the best results in their study, while in this study, the temperature was found to be 1600°C. In a separate study by the same authors²⁶, Al₂O₃-SiC composites were synthesized by pressure less sintering for 6h and 1600°C as the optimum conditions. Comparing their findings with those from this study, it is evident that Spark Plasma Sintering technique significantly decreases the amount of time required to achieve the optimum densification and mechanical properties. This has an advantage of achieving the desired properties with minimized grain growth, resulting in energy saving and superior mechanical properties, owing to the pressure assisted, rapid heating electric pulse mechanism applied in SPS technique.

3.6 Effects of SiC composition and sintering temperature on hardness

Figure 8 presents the effect of sintering temperature and SiC content on the hardness of Al₂O₃-SiC composites. It was observed that the hardness of the composites increased with SiC content at each respective sintering temperature.

This behavior could be attributed to the addition SiC phase that is harder²⁷ or, additionally, due to the refinement of the alumina matrix grains, where the composites with a higher SiC content tend to have smaller grains where dislocations' slips are blocked by grain boundaries. The refinement of alumina grains is shown in Figure 9 for Al₂O₃-SiC composites sintered at 1600°C, where the composites with 20 vol% SiC has a smaller grain size than the 5 vol% SiC content. For illustration purposes, the difference in grain size is shown in the figure. The average grain size reported by Párvodiakovský et al.²⁸, in a related study reported that there was no significant effect of SiC particle size on the hardness of the composites, but it is mainly affected by volume fraction of the second phase. Meanwhile, hardness was found to increase with an increase in sintering temperature for 10 vol% and 20 vol%. However, an unusual decrease was observed in hardness for the 5 vol% and 15 vol% as the temperature approached 1600°C. It is believed that at lower amounts of SiC, the growth of matrix grains was inhibited to a lesser extent resulting in larger grain sizes and consequently lower hardness values, while it was suppressed almost entirely at higher volume fractions of SiC resulting in higher hardness values even at higher temperatures. Comparing the hardness of the composites to that of pure alumina sintered at similar conditions as presented in Table 2, it is revealed that the addition of SiC to alumina matrix results in increased hardness values at higher volume fractions of SiC.

Table 1: Effect of SiC Reinforcement on the Relative Density of Sintered Composites

SiC content (vol.%)	1300°C	1400°C	1500°C	1600°C
	Relative density (%)			
0	98.4	98.6	100.0	100.0
5	88.9	98.0	100.0	99.8
10	93.0	96.0	99.1	100.0
15	100.0	100.0	100.0	100.0
20	84.6	93.9	96.4	99.7

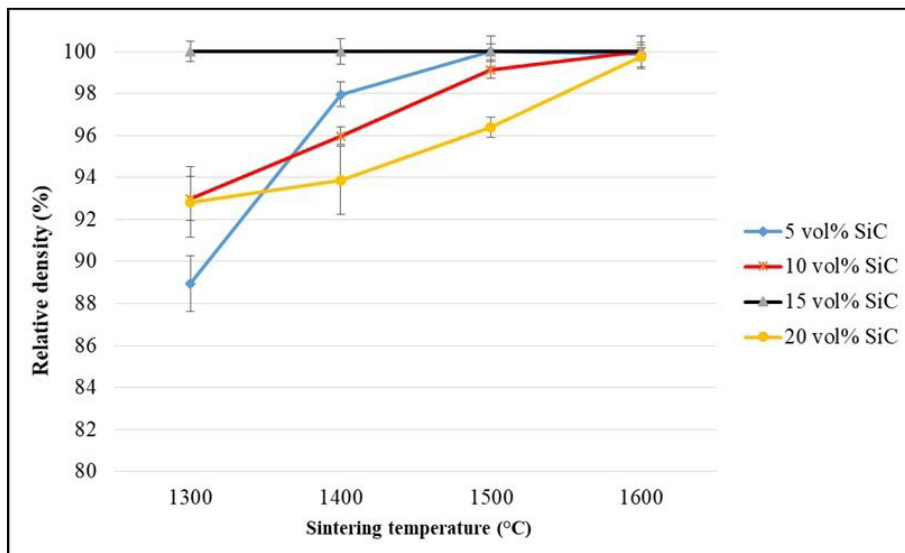


Figure 7: Relative density of Al₂O₃-SiC materials as a function of sintering temperature and SiC content

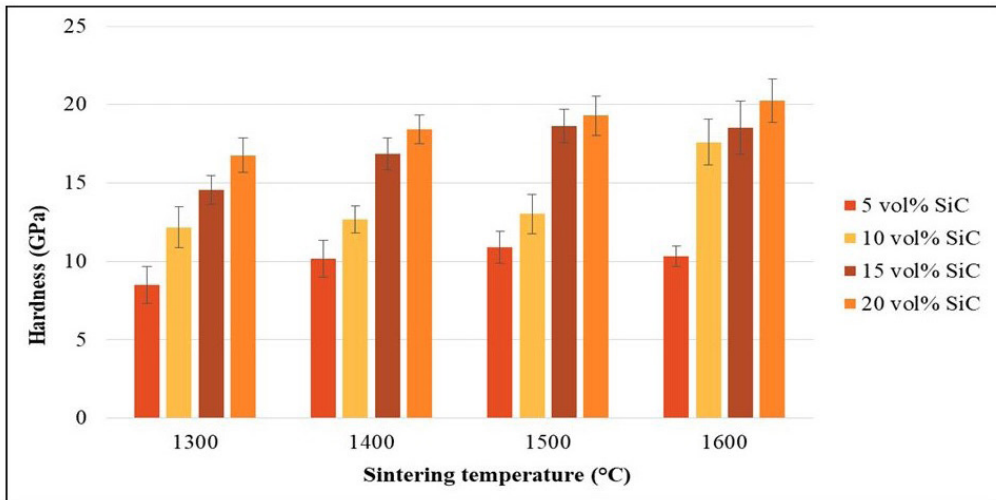


Figure 8: Hardness of Al_2O_3 -SiC composites as a function of sintering temperature

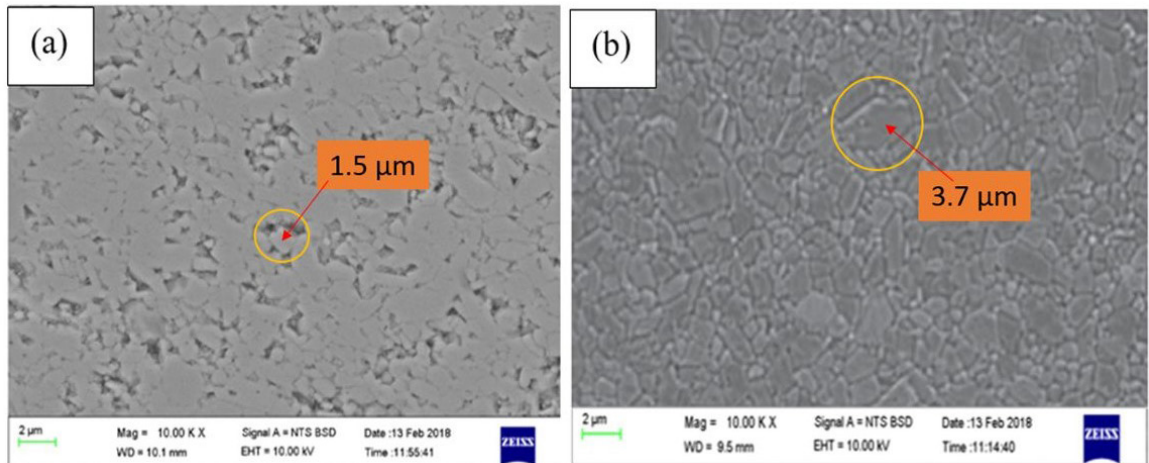


Figure 9: SEM images of Al_2O_3 -SiC composites sintered at 1600°C (a) 20vol.% SiC (b) 5vol.% SiC

Table 2: Effect of SiC Reinforcement on Hardness of Sintered Composites

SiC content (vol.%)	1300°C	1400°C	1500°C	1600°C
	Hardness (GPa)			
0	14.4	18.3	16.5	15.8
5	8.5	10.2	10.9	10.3
10	12.3	12.7	13.0	16.1
15	14.6	16.9	18.6	18.5
20	16.8	18.4	19.3	20.2

3.7 Effects of sintering temperature and SiC composition on fracture toughness

Figure 10 presents the effect of sintering temperature on the fracture toughness of various Al_2O_3 -SiC composites. There was not really a defined relationship between SiC content and fracture toughness observed. Parchovianský et al.²⁸, in a related study reported that the mechanism of fracture toughness of Al_2O_3 -SiC composites is complicated. There exists a widespread of theories published²⁹⁻³¹ on factors that

influence the fracture toughness of these composites such as the amount of SiC, the particle size of SiC, influence of intragranular and intergranular SiC phases, role of residual stresses and many more. It has however, been established that the mismatch in thermal expansion of Al_2O_3 ($8.8 \times 10^{-6} \text{ K}^{-1}$) and SiC ($4.4 \times 10^{-6} \text{ K}^{-1}$) causes the intergranular SiC phases to bond strongly at $\text{Al}_2\text{O}_3/\text{Al}_2\text{O}_3$ interfaces, which inhibits the propagation of cracks along grain boundaries, resulting in a change from intergranular to intragranular cracking³². The high fracture energy of $\text{Al}_2\text{O}_3/\text{SiC}$ interfaces of the intragranular

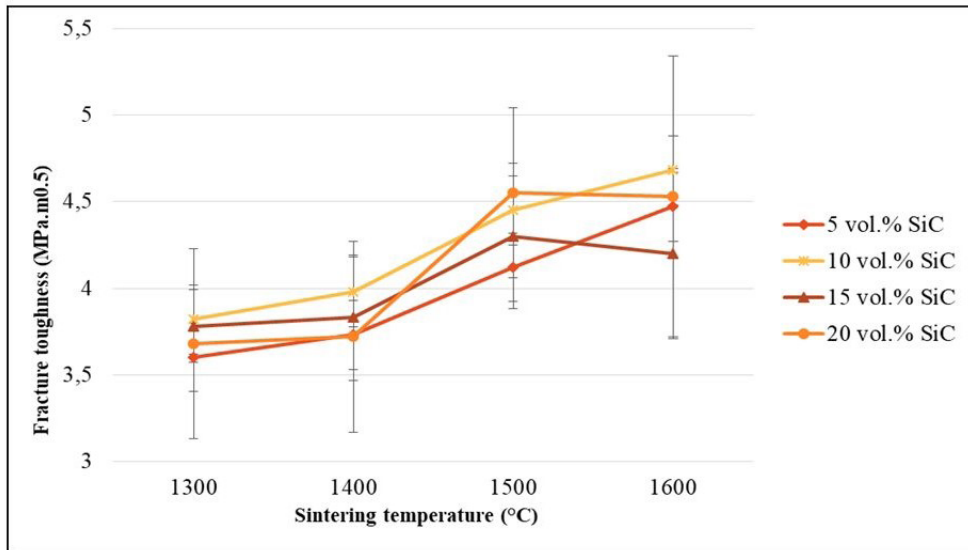


Figure 10: Fracture toughness of various compositions of Al_2O_3 -SiC materials as a function of sintering temperature

Table 3: Effect of SiC Reinforcement on the Fracture Strength of Sintered Composites

SiC content (vol.%)	1300°C	1400°C	1500°C	1600°C
	Fracture toughness ($\text{MPa}\cdot\text{m}^{0.5}$)			
0	3.2	3.6	3.6	4.2
5	3.6	3.7	4.1	4.5
10	3.8	4.0	4.5	4.7
15	3.8	3.8	4.3	4.2
20	3.7	3.7	4.1	4.2

SiC inclusions results in the deflection²⁸ of cracks. On the other hand, the mismatch in thermal expansion between Al_2O_3 and SiC results in circular compressive forces and tangential tensile forces to act on SiC particles. This implies that at lower amounts of SiC, part of the matrix is compressed while the other is under tension, hence, the propagation of cracks is inhibited in regions under compression while the tensile regions promote crack propagation. However, at higher amounts of SiC, the entire matrix becomes tensile, which leads to a promotion of crack propagation and lowering the fracture energy of the composites¹⁸. This explains why the fracture toughness of the composites was only improved at lower amounts of SiC and decreased at higher volume fractions. Meanwhile, It was observed that for low SiC content (5 and 10 vol%), the fracture toughness increased with sintering temperature. This may be attributed to the increase in fracture energy of Al_2O_3 /SiC interfaces caused by an increase in residual stresses experienced at higher temperatures. However, the fracture toughness decreased for higher SiC contents (15 and 20 vol%), which could be caused by embrittlement of the matrix due to microstructure refinement and prohibition of grain growth by the SiC particles. Comparing the fracture toughness values of the composites to those of pure alumina sintered at similar conditions as presented in Table 3, it is evident that the addition of SiC leads to improved fracture toughness, although the relationship between SiC volume fraction and fracture toughness is not well defined from the results. Perhaps, more research needs to be carried out to better define this relationship.

4. Conclusions

The synthesis of SiC from rice husk and the mechanical properties of alumina reinforced with SiC from rice husk were studied. The results showed that a maximum yield of 69.2% was achieved in this study. Analysis of the morphology of the synthesized SiC revealed that the powder was a mixture of particulates and whiskers in the nanometre range. The yield of SiC from rice husk was found to be dependent on the pyrolysis temperature and time. In addition, the morphology and mechanical behaviour of Al_2O_3 -SiC were studied. Density results showed that an increase in sintering temperature improved the densification, while beyond 15 vol% SiC, the densification decreased. Hardness improved with SiC content, but the fracture toughness only increased up to 10 vol%. The maximum values obtained in this work for both hardness and fracture toughness were 20.2 ± 1.4 GPa and 4.7 ± 0.7 $\text{MPa}\cdot\text{m}^{0.5}$, respectively. Rice husk has the potential to become an alternative source of low cost SiC that may lead to commercial production of low-cost ceramic materials.

5. Acknowledgements

The authors give acknowledgement to the African Materials Science and Engineering Network (AMSEN) for financial support, as well as the Institute of Nano-Engineering and Research (INER) at Tshwane University of Technology (TUT), Pretoria, South Africa for research collaboration.

6. References

- Ahmad K, Pan W. Microstructure-toughening relation in alumina based multiwall carbon nanotube ceramic composites. *J Eur Ceram Soc.* 2015;35(2):663-71.
- Li X, Gao M, Jiang Y. Microstructure and mechanical properties of porous alumina ceramic prepared by a combination of 3-D printing and sintering. *Ceram Int.* 2016;42(10):12531-5.
- Ando KK, Kim BS, Chu MC, Saito S, Takahashi K. Crack-healing and mechanical behaviour of Al₂O₃/SiC composites at elevated temperature. *Fatigue Fract Eng M.* 2004;27:533-41.
- Chen Y, Balani K, Agarwal A. Do thermal residual stresses contribute to the improved fracture toughness of carbon nanotube/alumina nanocomposites? *Scr Mater.* 2012;66(6):347-50.
- Hanzel O, Sedláček J, Šajgalík P. New approach for distribution of carbon nanotubes in alumina matrix. *J Eur Ceram Soc.* 2014;34(7):1845-51.
- Kasperski A, Weibel A, Estournès C, Laurent C, Peigney A. Multi-walled carbon nanotube-Al₂O₃ composites: covalent or non-covalent functionalization for mechanical reinforcement. *Scr Mater.* 2014;75:46-9.
- Niihara K, Jeong YK. Microstructure and mechanical properties of pressureless sintered Al₂O₃/SiC nanocomposites. *Nanostruct Mater.* 1997;9(8):193-6.
- Li J, Shirai T, Fujii M. Rapid carbothermal synthesis of nanostructured silicon carbide particles and whiskers from rice husk by microwave heating method. *Adv Powder Technol.* 2013;24(5):838-43.
- Shen Y, Zhao P, Shao Q. Porous silica and carbon derived materials from rice husk pyrolysis char. *Microporous Mesoporous Mater.* 2014;188:46-76.
- Taha AA, Ghani SAA. Adsorption kinetics, equilibrium, and thermodynamics of copper from aqueous solutions using silicon carbide derived from rice waste. *J. Disp. Sc. Tech.* 2016;37(2):173-82.
- Zawrah MF, Zayed MA, Ali MRK. Synthesis and characterization of SiC and SiC/Si₃N₄ composite nano powders from waste material. *J Hazard Mater.* 2012;228:250-6.
- Ali M, Tindyala MA. Thermoanalytical studies on acid-treated rice husk and production of some silicon based ceramics from carbonised rice husk. *J Am Ceram Soc.* 2015;3(3):311-6.
- Stachowicz L, Singh SK, Wender E, Girshick SL. Synthesis of ultrafine SiC from rice hulls (husks): a plasma process. *Plasma Chem Plasma Process.* 1993;13(3):447-61.
- Martínez V, Valencia MF, Cruz J, Mejía JM, Chejne F. Production of β-SiC by pyrolysis of rice husk in gas furnaces. *Ceram Int.* 2006;32(8):891-7.
- Gorzowski EP, Qadri SB, Rath BB, Goswami R, Caldwell JD. Formation of nanodimensional 3C-SiC structures from rice husks. *J Electron Mater.* 2013;42(5):799-804.
- Korablev SF, Korablev DS. Physicochemical features in the synthesis of nanostructured sic under nonisothermal heating from hydrothermally carbonized rice husk. II. Production of SiC without carbon impurities. *Powder Metall Met Ceramics.* 2015;54(3):215-9.
- Alaneme KK, Ekperusi JO, Oke SR. Corrosion behaviour of thermal cycled aluminium hybrid composites reinforced with rice husk ash and silicon carbide. *J King Saud Univ Eng Sc.* 2018;30:391-7.
- Tiwari S, Pradhan MK. Effect of rice husk ash on properties of aluminium alloys: a review. *Mater. Today-Proc.* 2017;4(2):486-95.
- Pattnayak A, Madhu N, Panda AS, Sahoo MK, Mohanta K. A Comparative study on mechanical properties of Al-SiO₂ composites fabricated using rice husk silica in crystalline and amorphous form as reinforcement. *Mater. Today-Proc.* 2018;5(2):8184-92. <http://dx.doi.org/10.1016/j.matpr.2017.11.507>.
- ASTM: American Society for Testing and Materials. ASTM D5373-02: test methods for instrumental determination of carbon, hydrogen, and nitrogen in laboratory samples of coal and coke. West Conshohocken: ASTM International; 2007.
- Alweendo S, Johnson O, Shongwe M, Kavishe F, Borode J. Synthesis, optimization and characterization of silicon carbide (SiC) from rice husk. *Procedia Manuf.* 2019;35:962-7.
- Anstis G, Chantikul P, Lawn B, Marshall D. A critical evaluation of indentation techniques for measuring fracture toughness: I, direct crack measurements. *J Am Ceram Soc.* 1981;64(9):533-8.
- Adylov GT, Faiziev SA, Paizullakhanov MS, Mukhsimov S, Nodirmatov E. Silicon carbide materials obtained from rice husk. *Tech Phys Lett.* 2003;29(3):221-3.
- Chandrasekhar S, Pramada PN, Majeed J. Effect of calcination temperature and heating rate on the optical properties and reactivity of rice husk ash. *J Mater Sci.* 2006;41(23):7926-33.
- Min X, Fang M, Huang Z, Jin G, Liu Y, Tang C, et al. Synthesis of Sialon-SiC composites from kyanite tailings by carbothermal reduction nitridation. *J Miner Met Mater Soc.* 2015;67(6):1379-84. <http://dx.doi.org/10.1007/s11837-015-1423-7>.
- Min X, Fang M, Huang Z, Chen J, Zhang J, Liu Y, et al. Preparation of Al₂O₃-SiC composite powder from kyanite tailings via carbothermal reduction process. *Adv Appl Ceramics.* 2018;117(1):9-15. <http://dx.doi.org/10.1080/17436753.2017.1362507>.
- Sedláček J, Galusek D, Švančárek P, Riedel R, Atkinson A, Wang X. Abrasive wear of Al₂O₃-SiC and Al₂O₃-(SiC)-C composites with micrometer- and submicrometer-sized alumina matrix grains. *J Eur Ceram Soc.* 2008;28(15):2983-93.
- Parchovianský M, Balko J, Švančárek P, Sedláček J, Dusza J, Lofaj F, et al. Mechanical properties and sliding wear behaviour of Al₂O₃-SiC nanocomposites with 3-20 vol% SiC. *J Eur Ceram Soc.* 2017;37(14):4297-306.
- Dong YL, Xu FM, Shi XL, Zhang C, Zhang ZJ, Yang JM, et al. Fabrication and mechanical properties of nano-/micro-sized Al₂O₃/SiC composites. *Mater Sci Eng A.* 2009;504(1-2):49-54.
- Shi XL, Xu FM, Zhang ZJ, Dong YL, Tan Y, Wang L, et al. Mechanical properties of hot-pressed Al₂O₃/SiC composites. *Mater Sci Eng A.* 2010;527(18-19):4646-9.
- Parchovianský M, Galusek D, Michálek M, Švančárek P, Kašiarová M, Dusza J, et al. Effect of the volume fraction of SiC on the microstructure and creep behavior of hot pressed Al₂O₃/SiC composites. *Ceram Int.* 2014;40(1):1807-14.
- Lv B, Zhang FC, Luo HH, Zhang M. Inter-phase microstress on the grain boundary in Al₂O₃/SiC nanocomposites. *Scr Mater.* 2011;64(3):260-3.